Int. J. Electrochem. Sci., 17 **(2022)** Article Number: 221155, doi: 10.20964/2022.11.52

International Journal of
ELECTROCHEMICAL
SCIENCE
www.electrochemsci.org

A Ratiometric Electrochemical Aptasensor with Exonuclease I-assisted Target Recycling Amplification for Highly Sensitive Detection of Carcinoembryonic Antigen

Ping Wang[*], *Huikai Ma, Yaoyao Xie, Sanqiang Li*[*]

School of Basic Medical Sciences, Henan University of Science and Technology, Luoyang 471000, China
[*]E-mail: glorywangping@163.com, sanqiangli2001@163.com

Received: 2 August 2022 / *Accepted:* 14 September 2022 / *Published:* 10 October 2022

In this study, a ratiometric electrochemical aptasensor was proposed for the highly sensitive detection of carcinoembryonic antigen (CEA) with exonuclease I (Exo I)-assisted target recycling amplification. The thiolated methylene blue (MB)-labelled hairpin capture probe (MB-HP) was immobilized on the surface of gold nanoparticles (AuNPs) modified gold electrode (AuE) via Au-S bonding, and the hybridization between MB-HP and ferrocene (Fc)-labelled aptamer (Fc-Apt) formed a duplex structure, leading to Fc molecules approaching to the electrode surface while MB molecules were far away. In the presence of CEA, its specific recognition with the aptamer caused the release of Fc-Apt from the electrode surface and subsequently the formation of a hairpin structure for MB-HP, resulting in both "signal-on" of MB (I_{MB}) and "signal-off" of Fc (I_{Fc}). To improve the sensitivity of the aptasensor, an Exo I-assisted target recycling amplification strategy was designed to achieve an amplified ratiometric signal. Under the optimal conditions, the proposed aptasensor showed a linear detection range from 10 pg mL^{-1} to 100 ng mL^{-1} with a detection limit of 4.1 pg mL^{-1}. Furthermore, the stability, reproducibility, selectively and real sample detection ability of the aptasensor were investigated and satisfactory results were obtained.

Keywords: Ratiometric electrochemical aptasensor; Exonuclease I; Signal amplification; Carcinoembryonic antigen; Detection

1. INTRODUCTION

Cancer is a great threat to human health worldwide. Early detection and diagnosis is the key to improve the survival rate of cancer patients. Tumor biomarkers are biological molecules such as DNA, RNA, proteins, lipids or metabolites [1]. These molecules are relevant to the occurrence and development of some cancers, and play vital roles in the early screening, diagnosis and prognosis of cancer [2]. Carcinoembryonic antigen (CEA) is a glycoprotein that was first discovered in human

colon cancer by Gold and Freedman in 1965 [3]. As a widely used tumor biomarker, CEA is associated with various types of malignant tumors, such as colorectal cancer [4], breast cancer [5], pancreatic cancer [6], cervical cancer [7] and lung cancer [8]. In normal humans, the serum CEA content is less than 5 ng mL^{-1}, and an increase in the CEA level indicates a risk of cancer. Therefore, it is of great importance to develop a rapid, convenient and sensitive analytical method for CEA detection in serum.

Various immunoassay methods based on antigen-antibody specific recognition have been established for the determination of CEA, including enzyme-linked immunosorbent assay (ELISA) [9], electrochemical [10], electrochemiluminescence (ECL) [11], colorimetric [12], photoelectrochemistry [13] and surface-enhanced Raman scattering (SERS) [14]. The sensitivity and selectivity of these immunoassay methods are highly dependent on the quality of the antibody. Meanwhile, the performance of antibodies is affected by a variety of factors, such as the storage temperature, pH and ionic strength [15]. All these conditions limit the applications of the antibody based analytical methods.

Aptamers are artificial single-stranded DNA (ssDNA) or RNA molecules screened by systematic evolution of ligands by exponential enrichment (SELEX) in vitro [16] that can bind to various targets with high affinity and specificity, such as proteins, nucleic acids or cells [17]. Compared with antibodies, aptamers have many advantages in terms of good stability, easy synthesis and convenient modification. Given these properties, aptamers have attracted researchers' interest as biorecognition elements for biosensors. A variety of aptasensors have been developed for the detection of CEA, such as electrochemical [18], chemiluminescence [19], colorimetric [20], surface plasmon resonance spectroscopy (SPR) [21] and fluorescent [17] methods. Among these, electrochemical aptasensors have attracted researchers' attention due to their low cost, fast response, easy operation, high sensitivity and suitability for miniaturization [22, 23].

Usually, most of the developed electrochemical aptasensors have only a single signal, and they can be divided into "signal-on" or "signal-off" modes by designing target-induced conformational changes on the electrode surface. Recently, the ratiometric electrochemical method combined with "signal-on" and "signal-off" strategies, has been developed owing to its high reproducibility, better selectivity, lower detection limit and wider linear range [24]. Li et al. [25] reported a sensitivity programmable ratiometric electrochemical aptasensor for the detection of aflatoxin B1 in peanut using thionine (THI) and ferrocene (Fc) as redox tags. Zhu et al. [26] developed a ratiometric electrochemical aptasensor for the ultrasensitive detection of ochratoxin A, which has great significance for mycotoxins monitoring in agricultural products and foods. To improve the sensitivity of detection, various signal amplification strategies have been developed, including hybridization chain reaction (HCR) [27, 28], rolling circle amplification (RCA) [29, 30], DNA walking machines [31, 32] and exonuclease (Exo)-assisted target recycling [33, 34]. Among them, Exo-assisted target recycling has been widely applied in the fabrication of electrochemical aptasensors due to the simplicity of equipment and ease of operation. Compared with nicking endonuclease, exonuclease does not require any specific recognition sequence [35] and thus has received increasing attention in target amplification detection. For example, Exo I is a sequence-independent enzyme that can catalyze the stepwise removal of mononucleotides from the 3' to 5' ends of ssDNA. Wen et al. [36] developed a sensitive exonuclease-assisted amplification electrochemical aptasensor for the detection of mucin 1,

and Exo I-assisted target recycling significantly amplified the electrochemical signal. Lin et al. [37] developed a sensitive and homogeneous electrochemical aptasensor for mucin 1 detection, and the usage of Exo I realized target recycling and caused amplification of the electrochemical signal.

Herein, we developed a CEA ratiometric aptasensor based on Exo I-assisted target recycling. The presence of CEA led to the dissociation of Fc modified aptamer DNA (Fc-Apt) from the electrode surface, and subsequently the formation of a hairpin structure of methylene blue (MB)-labelled capture DNA. Then, Exo I-assisted target recycling was triggered for CEA recycling. As a result, the electrochemical peak currents of MB (I_{MB}) and Fc (I_{Fc}) were dramatically increased and decreased with increasing of CEA concentrations, and the detection of CEA could be realized by monitoring the ratio of I_{MB}/I_{Fc}.

2. EXPERIMENTAL SECTION

2.1. Reagents

Hydrogen tetrachloroauratetrihydrate (HAuCl4·3H2O), Tris (2-carboxyethyl) phosphine (TCEP) and 6-mercapto-1-hexanol (MCH) were purchased from Shanghai Aladdin Biochemical Technology Co., Ltd (Shanghai, China). CEA, alpha-fetoprotein (AFP) antigen, human prostate specific antigen (PSA) and human serum albumin (HSA) were obtained from Shanghai Linc-Bio Science Co., Ltd. (Shanghai, China). Exo I and 10 × NEBuffer 3.1 were acquired from New England Biolabs Ltd. (Beijing, China). Ultrapure water (18.2 MΩ·cm) was used throughout the experiment.

All oligonucleotides with HPLC purification were obtained from Sangon Biological Engineering Technology & Co. Ltd. (Shanghai, China). The sequences are listed as follows:

MB-labelled hairpin capture probe (MB-HP):

5’-MB-AATTGAATAAGCTGGTATTTTTTTTTTGGATTCAATT-(HS-SH)-3’

Fc modified aptamer DNA (Fc-Apt):

5’-Fc-ATACCAGCTTATTCAATT-3’

2.2. Fabrication of the electrochemical aptasensor

The pretreatment of AuE and the electrodeposition of gold nanoparticles (AuNPs) on AuE were prepared according to our reported methods [38, 39]. First, 5 μL of MB-HP solution (10 μM) and 5 μL of TCEP (1 mM) were mixed for 1 h to allow the reduction of disulphide bonds. The mixture was diluted to 50 μL with I-buffer (10 mM Tris-HCl containing 1 mM EDTA, 100 mM NaCl and 10 mM TCEP, pH 7.4). Then, 5 μL of reduced MB-HP solution was added to the surface of AuNPs modified AuE at 4 °C for 12 h and rinsed with 10 mM Tris-HCl (pH 7.4). The electrode was then blocked with MCH (1 mM) for 1 h and washed. Next, the above electrode was incubated with Fc-Apt solution (1 μM) for 1 h at 37 °C. After rinsing with 10 mM Tris-HCl (pH 7.4), the resulting electrode was further incubated with different concentrations of CEA containing 10 U Exo I at 37 °C for 1 h. The electrode was rinsed and used for electrochemical measurements.

2.3. Measurement procedure

Cyclic voltammetry (CV) and electrochemical impedance spectroscopy (EIS) were performed on an Autolab PGSTAT 128N station (Metrohm Autolab, The Netherlands). Square-wave voltammetry (SWV) was carried out on a CHI840D electrochemical workstation (Chenhua Instruments Co., Shanghai, China). All electrochemical experiments were performed in a conventional three-electrode system. A modified gold electrode (AuE) was used as the working electrode. The Ag/AgCl electrode and the platinum wire were used as the reference electrode and the counter electrode, respectively. EIS and CV were performed in aqueous solution containing 5.0 mM $[Fe(CN)_6]^{3-/4-}$ and 0.1 M KCl. SWV was operated in E buffer in the potential range from - 0.4 to 0.6 V at a frequency of 25 Hz and a step potential of 4 mV.

3. RESULTS AND DISCUSSION

3.1. Working principle of the aptasensor

The principle of the proposed ratiometric electrochemical aptasensor for CEA detection was based on Exo I-assisted target recycling. As illustrated in **Figure 1**, a thiolated MB-labelled hairpin capture probe (MB-HP) was immobilized on the AuNPs modified AuE surface through typical Au-S bonds. After blocking the nonspecific binding sites with MCH, Fc-Apt was added and the hairpin structure of MB-HP was opened to form the MB-HP/Fc-Apt duplex. As a result, Fc was close to the electrode surface, whereas MB was away from the electrode surface.

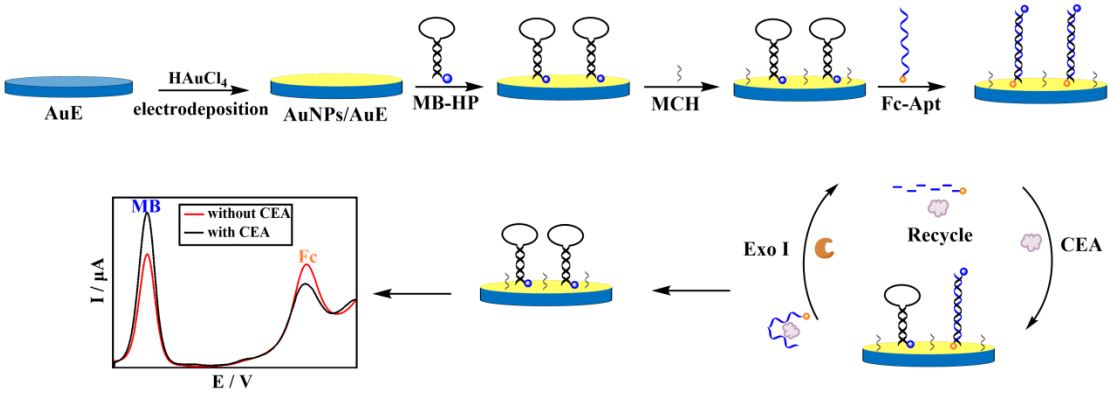

Figure 1. Schematic illustration of the ratiometric electrochemical aptasensor for highly sensitive detection of CEA with an Exo I-assisted target recycling amplification strategy.

In the presence of CEA, the binding ability of Fc-Apt to CEA was greater than that to MB-HP [40], which led to the disassociation of Fc-Apt from the MB-HP/Fc-Apt duplex, resulting in a decrease in the Fc signal. At the same time, MB-HP was transformed into a hairpin structure, and the MB signal increased. Exo I could digest Fc-Apt which made CEA participate in the next cycle, leading to the amplification of signals. In this way, the electrochemical peak currents of MB (I_{MB}) and Fc (I_{Fc}) were significantly increased and decreased, respectively. As a result, “signal-on” and “signal-off” elements

for dual-signal electrochemical ratiometric readout were achieved, and CEA concentrations could be monitored by measuring the change in I_{MB}/I_{Fc}.

3.2. Feasibility of the aptasensor

To demonstrate the feasibility of the developed aptasensor, SWV responses of the aptasensor under various conditions were investigated. As shown in **Figure 2**, two peaks at 0.392 V and - 0.260 V were observed without the addition of Exo I and CEA (curve a), which were assigned to the oxidation of Fc and MB, respectively. When only Exo I was present (curve b), the peak currents of Fc and MB were almost the same as curve a, indicating that Fc-Apt could not be digested by Exo I. When only CEA was present (curve c), the oxidation peak current of Fc decreased and that of MB increased. Such changes were due to the binding between Fc-Apt and CEA leading to the disassociation of Fc-Apt from the Fc-Apt/MB-HP duplex. When both CEA and Exo I were present in the system, the oxidation peak current of Fc decreased and that of MB increased obviously (curve d), which was ascribed to Exo I-assisted target recycling leading to a cascade amplification of electrochemical signals [41, 42]. These results demonstrated that the fabricated aptasensor could be used for the ratiometric detection of CEA.

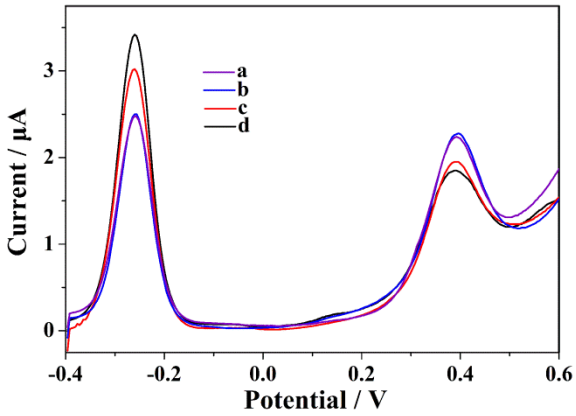

Figure 2. SWV responses of the constructed aptasensor under different conditions: (a) no CEA, no Exo I; (b) 10 U Exo I only; (c) 10 ng mL^{-1} CEA only; (d) 10 ng mL^{-1} CEA, 10 U Exo I.

3.3. Characterization of the developed aptasensor

EIS was employed to characterize the stepwise modification procedure. As shown in **Figure 3A**, the bare AuE (curve a) showed a small electron transfer resistance (R_{et}). The R_{et} of AuNPs/AuE significantly decreased, indicating that the AuNPs could improve the conductivity and electron transfer ability of the electrode interface. When MB-HP (curve c), MCH (curve d) and Fc-Apt (curve e) were modified on the electrode stepwise, the R_{et} value successively increased due to the obstruction of MCH, and these modifications could hinder the electron transfer process. However, the R_{et} value decreased after incubation with CEA (curve f), indicating that Fc-Apt was bound with CEA to release Fc-Apt from the electrode surface. The R_{et} value further decreased after coincubation with CEA and Exo I (curve g), probably because the Fc-Apt-CEA complex could be cleaved by Exo I and CEA was

detached and reused to react with Fc-Apt on the electrode. These results confirmed the successful construction of the aptasensor.

CV measurements were also performed to further confirm the process of electrode modification. As shown in **Figure 3B**, the peak current of AuNPs modified AuE (curve b) was obviously higher than that of bare AuE (curve a), which was ascribed to the well conductivity of AuNPs. After the immobilization of MB-HP, MCH and Fc-Apt, an obviously decreased current intensity was obtained (curves c, d and e, respectively). However, the current intensity increased after incubation with CEA (curve f) and further significantly increased when incubated with both CEA and Exo I (curve g). These results were consistent with the EIS characterization. All these results demonstrated the successful fabrication of the aptasensor.

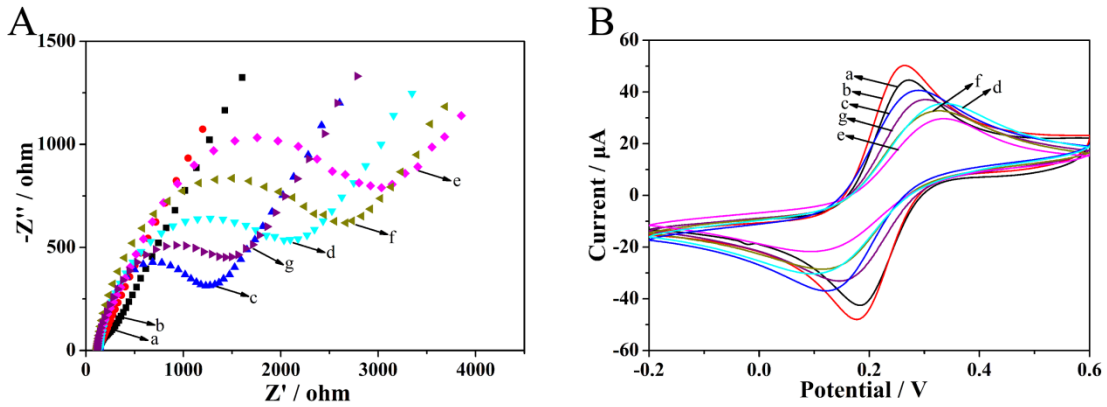

Figure 3. EIS (A) and CV (B) of the different modified electrodes in 0.1 M KCl solution containing 5 mM $[Fe(CN)_6]^{3-/4-}$: bare Au (a); AuE/Au (b); MB-HP/AuE/Au (c); MCH/Fc-HP2/AuE/Au (d); Fc-Apt/MCH/MB-HP/AuE/Au (e); Fc-Apt/MCH/MB-HP/AuE/Au incubated with 1 ng mL^{-1} CEA (f); Fc-Apt/MCH/MB-HP/AuE/Au incubated with 1 ng mL^{-1} CEA and 10 U Exo I (g).

3.4. Optimization of the experimental conditions

To achieve excellent performance, some experimental conditions, including the concentration of MB-HP, dosage of Exo I and incubation time of Exo I were optimized.

The concentration of MB-HP immobilized on the electrode could intensely influence the analytical performance of the developed ratiometric aptasensor. A lower concentration would reduce the detection sensitivity, while a higher concentration may cause steric hindrance and electrostatic repulsion, reducing the ability of MB-HP to form hairpin structures on the electrode. As shown in **Figure 4A**, the value of I_{MB}/I_{Fc} increased with increasing MB-HP concentrations from 0.2 to 1.0 μM and then slightly decreased. Therefore, 1.0 μM MB-HP was selected as the optimized concentration.

The effect of Exo I dosage was also assessed. As shown in **Figure 4B**, the value of I_{MB}/I_{Fc} increased with increasing Exo I dosage from 0 to 10 U and reached a plateau at 10 U. Therefore, 10 U was selected as the optimal reaction dosage in the subsequent assays.

The incubation time of Exo I was also an important parameter for the performance of the aptasensor. As shown in **Figure 4C**, the value of I_{MB}/I_{Fc} increased with increasing incubation time and

became stable at 60 min, indicating the completion of the digestion process. Thus, 60 min was chosen as the optimal incubation time in this work.

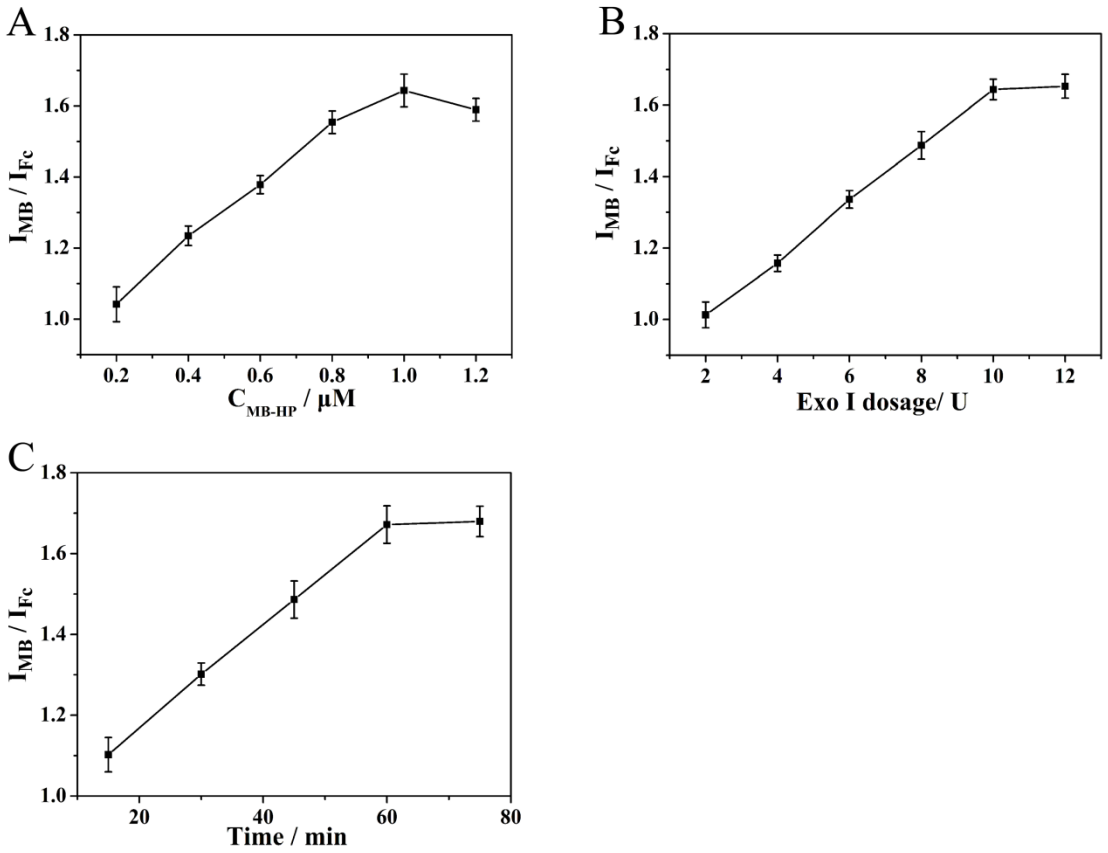

Figure 4. Optimization of the assay conditions: (A) the concentration of MB-HP, (B) dosage of Exo I and (C) incubation time of Exo I. The error bars represent the standard deviation of three measurements.

3.5. Determination of CEA

Under the optimal experimental conditions, SWV was used to detect different concentrations of CEA. As presented in **Figure 5A**, with increasing CEA concentration, I_{MB} gradually increased and I_{Fc} gradually decreased. A linear relationship between the value of I_{MB}/I_{Fc} and the logarithmic concentration of CEA in the range from 10 pg mL^{-1} to 100 ng mL^{-1} is plotted in **Figure 5B**. The linear regression equation was I_{MB}/I_{Fc} = 1.6099 + 0.2371 log C (ng mL^{-1}) with a linear regression coefficient of 0.9975, and the detection limit was calculated to be 4.1 pg mL^{-1} [43]. A comparison between our proposed method and other reported aptasensors [44-49] for CEA detection is listed in **Table 1**. Compared with these methods, our strategy had an improved or comparable detection limit and linear range. The excellent performance of the aptasensor was attributed to the following aspects. First, the electrodeposition of AuNPs on the AuE surface could provide a larger electroactive surface area and showed better electroconductivity [50]. Second, the dual-signal design increased the detection sensitivity and accuracy. Third, the Exo I-assisted target recycling strategy could amplify the detection signal.

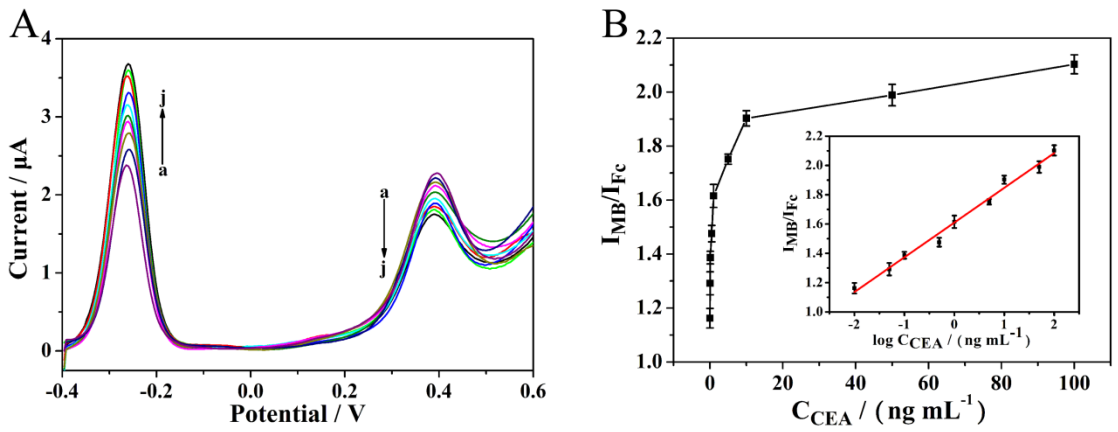

Figure 5. (A) SWV responses of different CEA concentrations (from curve a-j: 0, 10 pg mL^{-1}, 50 pg mL^{-1}, 100 pg mL^{-1}, 500 pg mL^{-1}, 1 ng mL^{-1}, 5 ng mL^{-1}, 10 ng mL^{-1}, 50 ng mL^{-1}, 100 ng mL^{-1}). (B) Calibration plot between I_{MB}/I_{Fc} and the concentrations of CEA. Inset: linear relationship between I_{MB}/I_{Fc} and the logarithm of CEA concentrations. The error bars represent the standard deviation of three measurements.

Table 1. Comparison between our strategy and other aptasensors for CEA detection.

Analytical method	Linear range	Detection limit	References
Colorimetric	1 ng mL^{-1} to 50 ng mL^{-1}	1 ng mL^{-1}	[44]
Fluorescence	0.05 ng mL^{-1} to 20 ng mL^{-1}	6.7 pg mL^{-1}	[45]
Fluorescence	0.03 ng mL^{-1} to 6 ng mL^{-1}	7.9 pg mL^{-1}	[46]
Chemiluminescence	65.4 pg mL^{-1} to 6.54 ng mL^{-1}	4.8 pg mL^{-1}	[47]
Electrochemical	10 pg mL^{-1} to 40 ng mL^{-1}	3.6 pg mL^{-1}	[48]
Electrochemical	10 pg mL^{-1} to 5 ng mL^{-1}	4.8 pg mL^{-1}	[49]
Electrochemical	10 pg mL^{-1} to 100 ng mL^{-1}	4.1 pg mL^{-1}	This work

3.6. Selectivity, reproducibility and stability of the aptasensor

To assess the selectivity of the ratiometric electrochemical aptasensor, three interferences PSA, HSA and AFP, with concentrations 10-fold higher than that of CEA (1 ng mL^{-1}) were detected along with CEA. As shown in **Figure 6**, the value of I_{MB}/I_{Fc} in the presence of CEA was obviously higher than that in the presence of interferences. In addition, when the aptasensor was incubated with 1 ng mL^{-1} CEA and 10 ng mL^{-1} of the three interferents, the value of I_{MB}/I_{Fc} showed no obvious change in comparison with that of only CEA. These results indicated the high selectivity of the aptasensor for CEA detection.

The reproducibility of the developed aptasensor was evaluated by measuring six parallels of the aptasensors in the presence of 1 ng mL^{-1} CEA. The relative standard deviation (RSD) was 2.90%, showing the good reproducibility of the aptasensor. Moreover, the stability of the aptasensor was demonstrated by storing the aptasensor at 4 °C for two weeks, 87.8% of the initial current response was obtained, indicating its good stability.

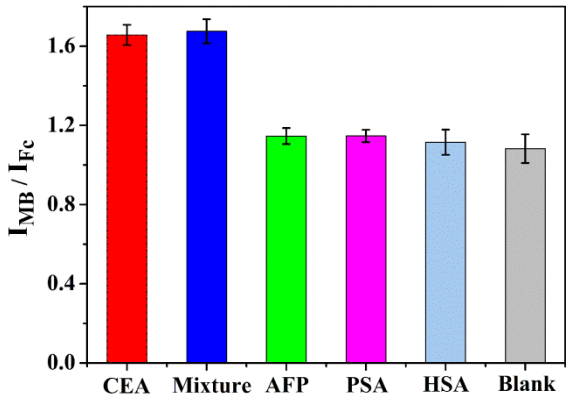

Figure 6. The selectivity of the aptasensor for various interferences. The error bars represent the standard deviation of three measurements.

3.7. Clinical serum sample analysis

The practical application of the aptasensor was determined by recovery experiments. The human serum samples (supported by the volunteers from Henan University of Science and Technology Hospital, diluted 10-fold with 20 mM PBS before use) were spiked with CEA at different concentrations. As shown in **Table 2**, the recoveries of the spiked samples were 96.0-102.8%, and the RSDs ranged from 1.89% to 4.26%, implying that the proposed aptasensor has great potential for the analysis of CEA in clinical samples.

Table 2. Application of the proposed aptasensor for CEA detection in diluted human serum samples.

Sample	Added CEA (ng mL^{-1})	Detected CEA (ng mL^{-1})	Recovery (%)	RSD (%)
1	10.00	10.28	102.8	2.81
2	5.00	5.11	102.2	1.89
3	1.00	0.96	96.0	4.26

4. CONCLUSIONS

In summary, we developed a novel ratiometric electrochemical aptasensor for CEA detection with an Exo I-assisted target recycling amplification strategy. The specific binding between CEA and the aptamer resulted in a “signal-on” and “signal-off” change for the dual-signal electrochemical ratiometric readout, and an Exo I-assisted target recycling amplification strategy was designed to improve the detection sensitivity of the aptasensor. The proposed aptasensor was systematically optimized with the concentration of MB-HP, dosage of Exo I and incubation time of Exo I. As a result, a linear detection range from 10 pg mL^{-1} to 100 ng mL^{-1} and a detection limit of 4.1 pg mL^{-1} was

achieved. The aptasensor has been applied to detect CEA in human serum samples and obtained satisfactory results. In addition, the developed aptasensor possessed high sensitivity, good selectivity and stability, and could be adopted to detect various targets by changing the aptamer sequences.

References

1. K. Mäbert, M. Cojoc, C. Peitzsch, I. Kurth and S. Souchelnytskyi, A. Dubrovska, *Int. J. Radiat. Biol.*, 90 (2014) 659.
2. J. Jiang, J. Xia, Y. Zang and G. Diao, *Sensors*, 21 (2021) 7742.
3. P. Gold and S.O. Freedman, *J. Exp. Med.*, 121 (1965) 439.
4. J.N. Primrose, R. Perera, A. Gray, P. Rose, A. Fuller, A. Corkhill, S. George, D. Mant and F.T. Investigators, *Jama*, 311 (2014) 263.
5. S.G. Wu, Z.Y. He, J. Zhou, J.Y. Sun, F.Y. Li, Q. Lin, L. Guo and H.X. Lin, *The Breast*, 23 (2014) 88.
6. X. Ni, X. Bai, Y. Mao, Y. Shao, J. Wu, Y. Shan, C. Wang, J. Wang, Y. Tian and Q. Liu, *Eur. J. Surg. Oncol.*, 31 (2005) 164.
7. Malkin, J.A. Kellen, G.M. Lickrish and R.S. Bush, *Cancer*, 42 (1978) 1452.
8. M. Grunnet and J.B. Sorensen, *Lung Cancer*, 76 (2012) 138.
9. S. Yokoyama, A. Takeuchi, S. Yamaguchi, Y. Mitani and H. Yamaue, *PLoS One*, 12 (2017) e0183337.
10. X. Gu, Z. She, T. Ma, S. Tian and H.B. Kraatz, *Biosens. Bioelectron.*, 102 (2018) 610.
11. X. Zheng, G. Mo, Y. He, D. Qin, X. Jiang, W. Mo and B. Deng, *J. Electroanal. Chem.*, 844 (2019) 132.
12. M. Liu, C. Jia, Q. Jin, X. Lou, S. Yao, J. Xiang and J. Zhao, *Talanta*, 81 (2010) 1625.
13. Q. Han, R. Wang, B. Xing, T. Zhang, M.S. Khan, D. Wu and Q. Wei, *Biosens. Bioelectron.*, 99 (2018) 493.
14. H. Chon, S. Lee, W.S. Sang, C.H. Oh and J. Choo, *Anal. Chem.*, 81 (2009) 3029.
15. L. Huang, J. Wu, L. Zheng, H. Qian, F. Xue, Y. Wu, D. Pan, S.B. Adeloju and W. Chen, *Anal. Chem.*, 85 (2013) 10842.
16. R. Stoltenburg, C. Reinemann and B. Strehlitz, *Biomol. Eng.*, 24 (2007) 381.
17. Y. Bai, H. Zhang, L. Zhao, Y. Wang, X. Chen, H. Zhai, M. Tian, R. Zhao, T. Wang and H. Xu, *Talanta*, 221 (2021) 121451.
18. J.Y. Huang, L. Zhao, W. Lei, W. Wen, Y.J. Wang, T. Bao, H.Y. Xiong, X.H. Zhang and S.F. Wang, *Biosens. Bioelectron.*, 99 (2018) 28.
19. R. Han, Y. Sun, Y. Dai, D. Gao, X. Wang and C. Luo, *Sens. Actuators, B*, 326 (2021) 128833.
20. L. Yang, M. Cui, Y. Zhang, L. Jiang, H. Liu and Z. Liu, *Sens. Actuators, B*, 350 (2022) 130857.
21. C. Guo, F. Su, Y. Song, B. Hu, M. Wang, L. He, D. Peng and Z. Zhang, *ACS Appl. Mater. Interfaces*, 9 (2017) 41188.
22. H. Shu, W. Wen, H. Xiong, X. Zhang and S. Wang, *Electrochem. Commun.*, 37 (2013) 15.
23. L. Xu, Z. Liu, S. Lei, D. Huang and B. Ye, *Microchim. Acta*, 186 (2019) 473.
24. T. Yang, R. Yu, S. Liu, Z. Qiu, S. Luo, W. Li and K. Jiao, *Sens. Actuators, B*, 267 (2018) 519.
25. Y. Li, D. Liu, C. Zhu, X. Shen, Y. Liu and T. You, *J. Hazard. Mater.*, 387 (2020) 122001.
26. C. Zhu, D. Liu, Y. Li, X. Shen, S. Ma, Y. Liu and T. You, *Biosens. Bioelectron.*, 150 (2020) 111814.
27. L. Wang, L. Zeng, Y. Wang, T. Chen, W. Chen, G. Chen, C. Li and J. Chen, *Sens. Actuators, B*, 332 (2021) 129471.
28. L. Chen, L. Sha, Y. Qiu, G. Wang, H. Jiang and X. Zhang, *Nanoscale*, 7 (2015) 3300.
29. B. Shen, J. Li, W. Cheng, Y. Yan, R. Tang, Y. Li, H. Ju and S. Ding, *Microchim. Acta*, 182 (2015) 361.
30. P. Tong, W.W. Zhao, L. Zhang, J.J. Xu and H.Y. Chen, *Biosens. Bioelectron.*, 33 (2012) 146.

31. Y. Wang, W. Song, H. Zhao, X. Ma and T. Yue, *Biosens. Bioelectron.*, 182 (2012) 113171.
32. X. Yang, D. Shi, S. Zhu, B. Wang, X. Zhang and G. Wang, *ACS Sens.*, 3 (2018) 1368.
33. Z. Yan, N. Gan, T. Li, Y. Cao and Y. Chen, *Biosens. Bioelectron.*, 78 (2016) 51.
34. T. Bao, H. Shu, W. Wen, X. Zhang and S. Wang, *Anal. Chim. Acta*, 862 (2015) 64.
35. E. Xiong, X. Yan, X. Zhang, Y. Liu, J. Zhou and J. Chen, *Biosens. Bioelectron.*, 87 (2017) 732.
36. W. Wen, R. Hu, T. Bao, X. Zhang and S. Wang, *Biosens. Bioelectron.*, 71 (2015) 13.
37. C. Lin, H. Zheng, Y. Huang, Z. Chen, F. Luo, J. Wang, L. Guo, B. Qiu, Z. Lin and H. Yang, *Biosens. Bioelectron.*, 117 (2018) 474.
38. H. Ma, P. Wang, Y. Xie, J. Liu, W. Feng and S. Li, *Anal. Biochem.*, 649 (2022) 114694.
39. P. Wang, H. Ma, Y. Zhu, W. Feng, M. Su, S. Li and H. Mao, *J. Electroanal. Chem.*, 910 (2022) 116167.
40. X. Liang, F. Zhao, C. Xiao, S. Yue, Y. Huang and M. Wei, *J. Chin. Chem. Soc.*, 68 (2021) 1271.
41. G. Xu, J. Hou, Y. Zhao, J. Bao, M. Yang, H. Fa, Y. Yang, L. Li, D. Huo and C. Hou, *Sens. Actuators, B*, 287 (2019) 428.
42. H. Cui, K. An, C. Wang, Y. Chen, S. Jia, J. Qian, N. Hao, J. Wei and K. Wang, *Sens. Actuators, B*, 355 (2022) 131238.
43. C. Gan, L. Ling, Z. He, H. Lei and Y. Liu, *Biosens. Bioelectron.*, 78 (2016) 381.
44. N. Shahbazi, S. Hosseinkhani and B. Ranjbar, *Sens. Actuators, B*, 253 (2017) 794.
45. Z. Qiu, J. Shu and D. Tang, *Anal. Chem.*, 89 (2017) 5152.
46. Wang Y, Wei Z, Luo X, Wan Q, Qiu R and Wang S, *Talanta*, 195(2019)33.
47. Z.M. Zhou, Z. Feng, J. Zhou, B.Y. Fang, X.X. Qi, Z.Y. Ma, B. Liu, Y.D. Zhao and X.B. Hu, *Biosens. Bioelectron.*, 64 (2015) 493.
48. Z. Qiu, J. Shu, J. Liu and D. Tang, *Anal. Chem.*, 90 (2018) 1021.
49. Z. Qiu, J. Shu, J. Liu and D. Tang, *Anal. Chem.*, 91 (2018) 1260.
50. X. Chen, J. Huang, S. Zhang, F. Mo, S. Su, Y. Li, L. Fang, J. Deng, H. Huang and Z. Luo, ACS Appl. Mater. Interfaces, 11 (2019) 3745.